Supporting Information

Synthesis of an aggregation-induced emission (AIE) active salicylaldehyde based Schiff base: study of mechanoluminescence and sensitive Zn(II) sensing

Sheik Saleem Pasha[a], Hare Ram Yadav[b], Angshuman Roy Choudhury[b] and Inamur Rahaman Laskar[a]*

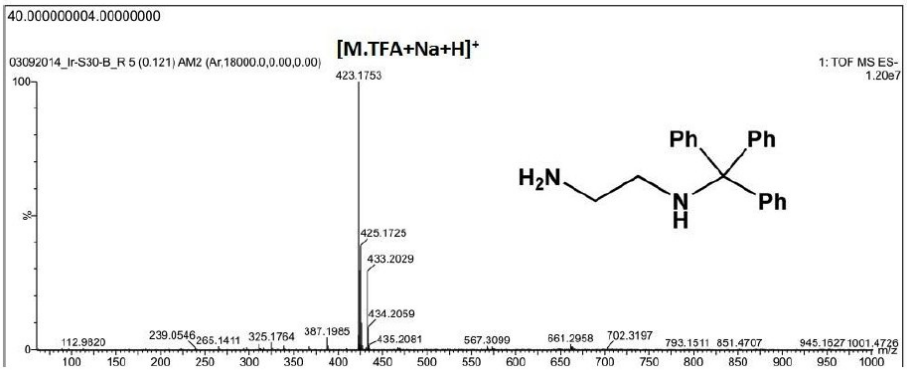

a

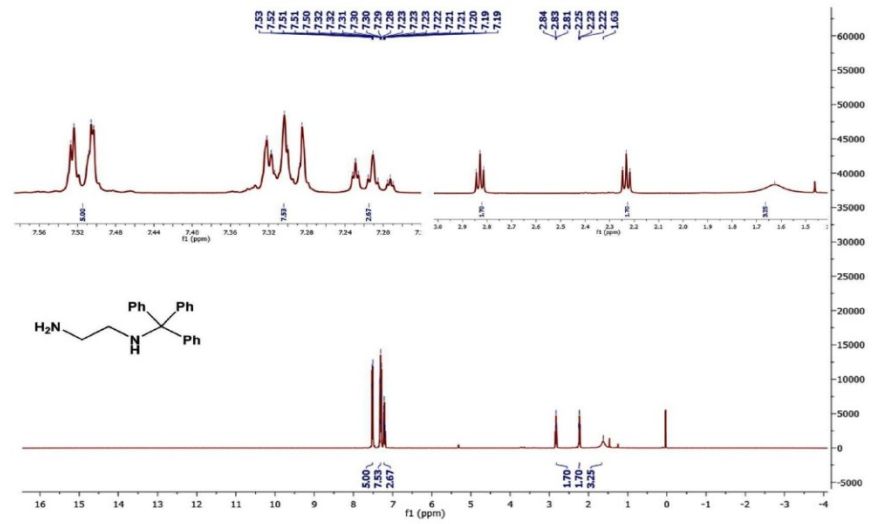

b

Fig. S1 a) HRMS data of **1** and b) ^{1}H NMR spectra of **1**

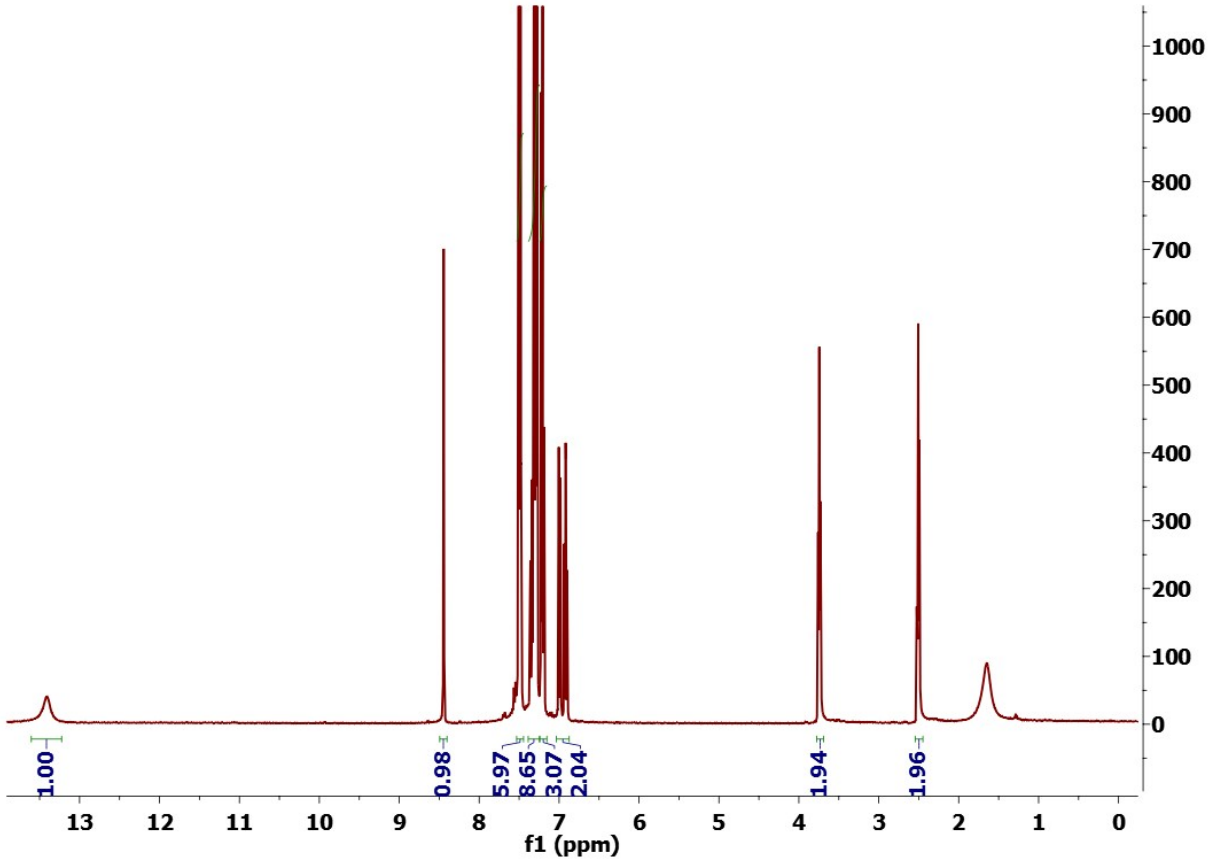

Fig. S2 ^{1}H NMR of **2**

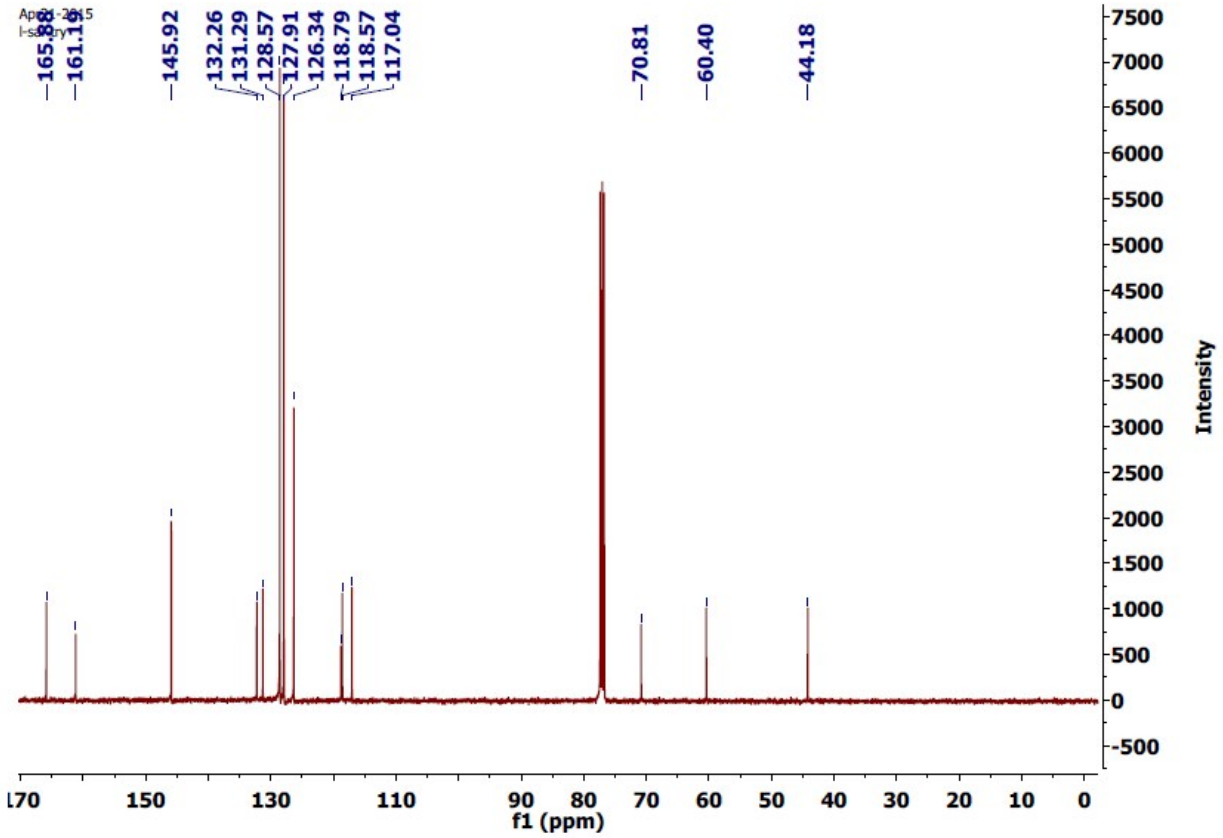

Fig. S3 ^{13}C NMR of **2**

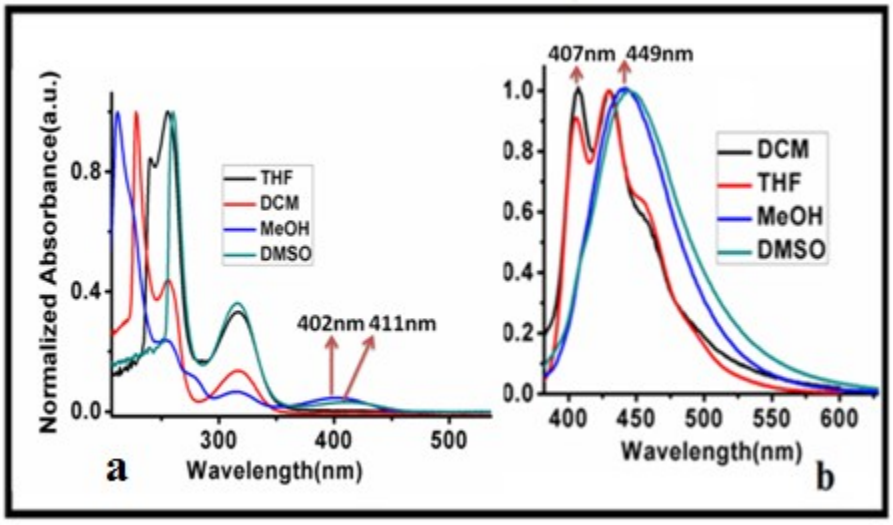

Fig. S4 a) Absorbance and b)photoluminescence spectra (exc. 365nm) of **2** in solvents with different polarity [tetrahydrofuran (THF); dichloromethane (DCM); methanol (MeOH); dimethylsulphoxide (DMSO)] at a concentration, $1x10^{-5}$M.

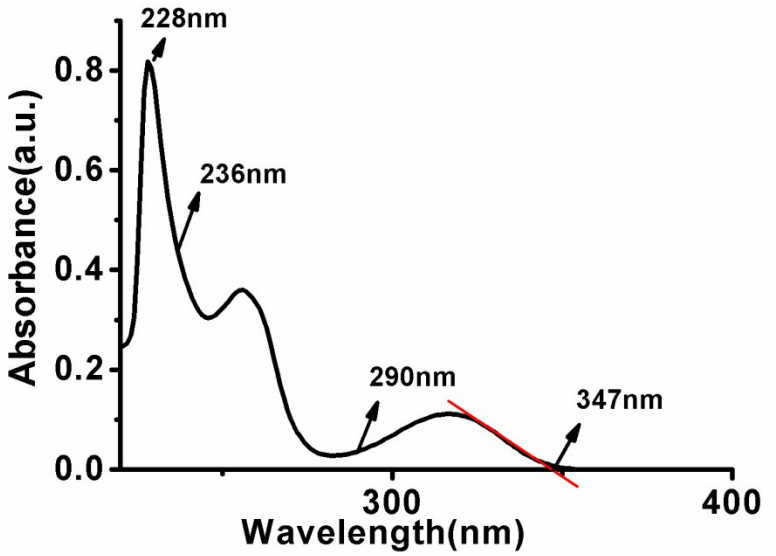

Fig. S5 a) Absorbance of **2** in DCM at a concentration, $1x10^{-5}$M.

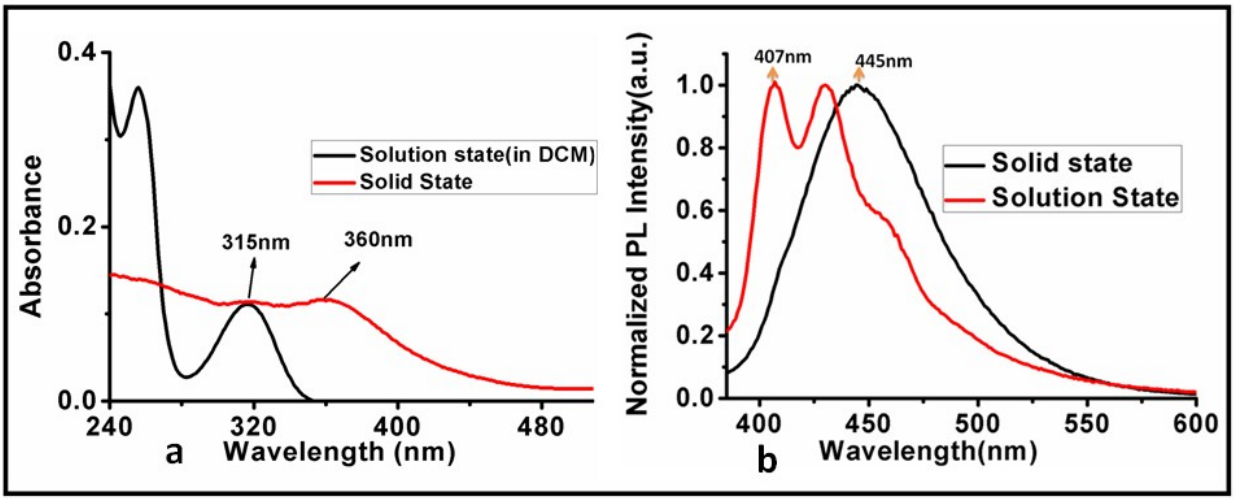

Fig. S6a) Shows absorbance spectra of **2** in solution(in DCM conc$1x10^{-5}$M) and solid state; b) Shows emission spectra of **2** in solution(in DCM conc $1X10^{-5}$M) state and solid state.

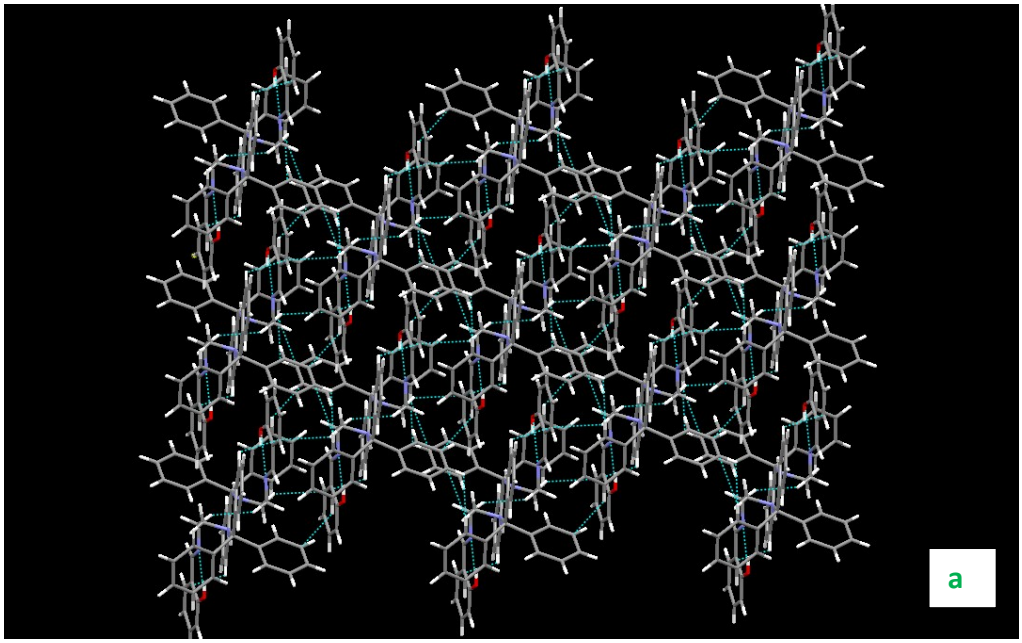
a

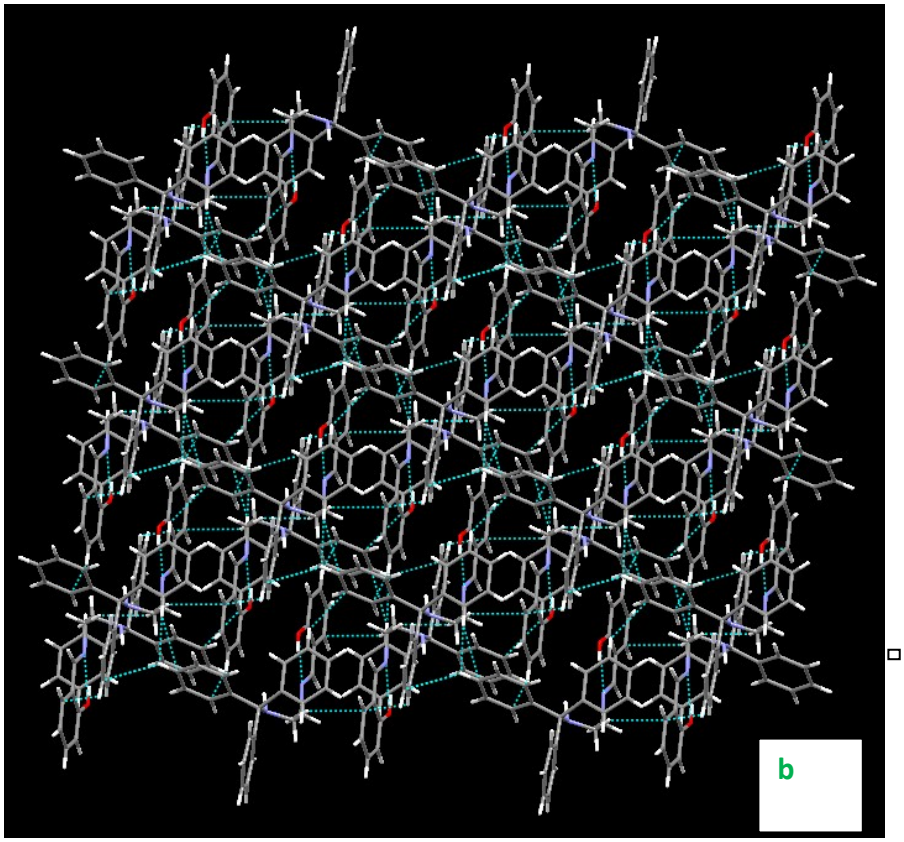
b

Fig. S7 a) It shows packing diagram of **2** at room temperature; b shows packing diagrams of **2** at liq. N_2 temperature (interaction shown in Figure in Å unit)

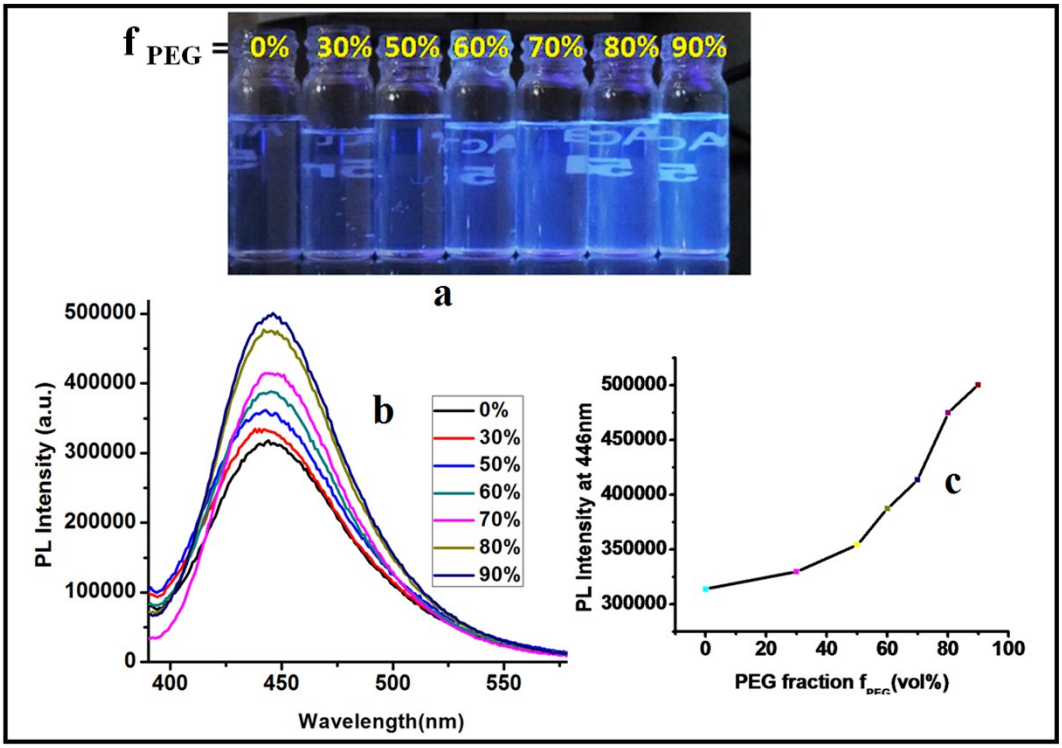

Fig .S8(a) Luminescent images of **2** (irradiated at 365nm by UV lamp); (b) PL spectra of **2** in MeOH/PEG mixed solvents with different fraction of PEG (f_{PEG}) with exciting at 365nm; (c) Plot of PL peak intensity change with different fraction of PEG in PEG-MeOH mixed solvents (f_{PEG}) (λ_{max} =449 nm) keeping the conc. 2×10^{-5} M.

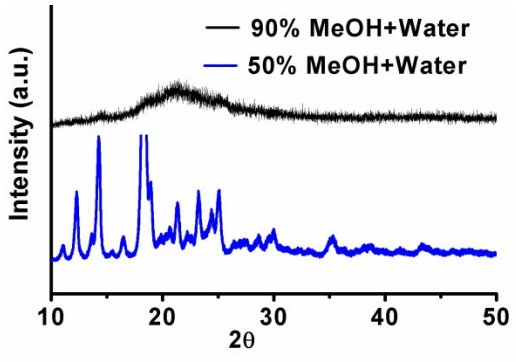

Fig. S9 Powder XRD of 2.

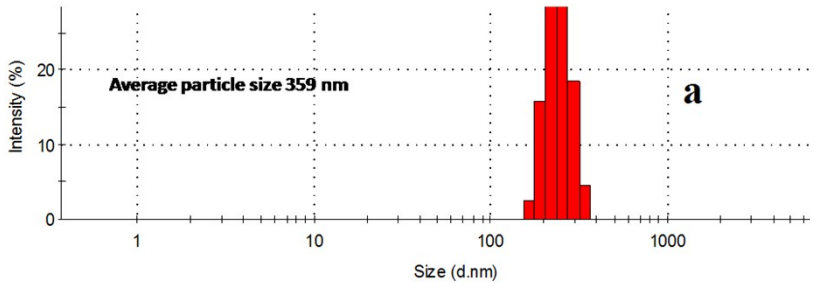

Fig.S10 Average particle size distribution of **2** at 50% methanol volume fractions in MeOH/Water.

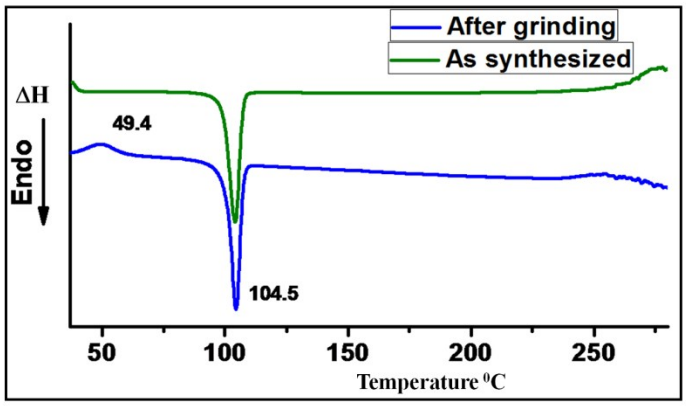

Fig. S11 DSC curve of **2** before grinding (green) and after grinding (blue) (glass transition temperature, 49.4ºC; melting temperature, 104.5ºC)

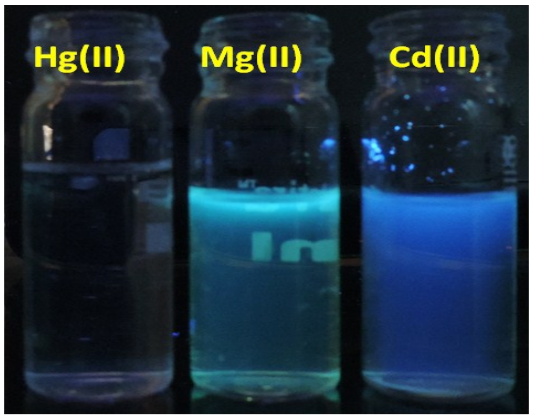

Fig. S12 Luminescent images of 2 in methanol (c, 1X10^{-5}M) with various metal salts($HgCl_2$, $Mg(NO_3)2$ and , $Cd(NO_3)_2$] (10 equiv., λexc. 365 nm) stirred for 15 minutes at 70°C.

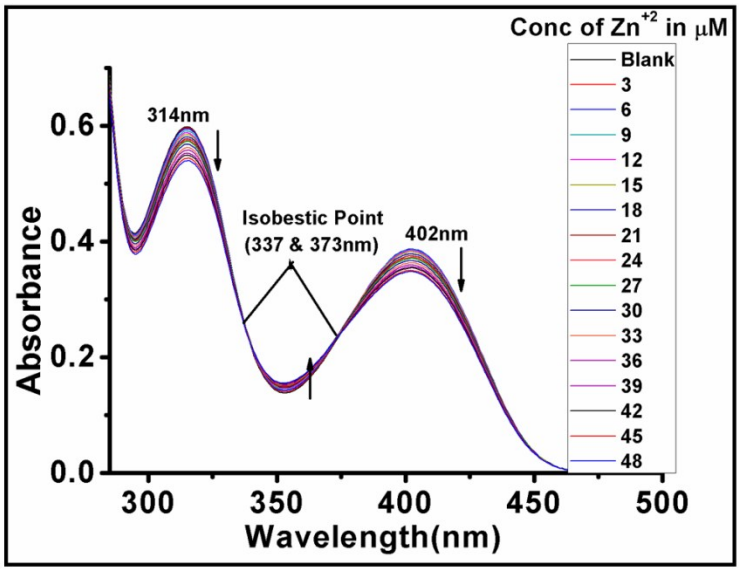

Fig. S13 Absorbance spectra of **2** in MeOH(conc. 1x10^{-5}M) with gradual increasing concentration of $Zn(NO_3)_2$.

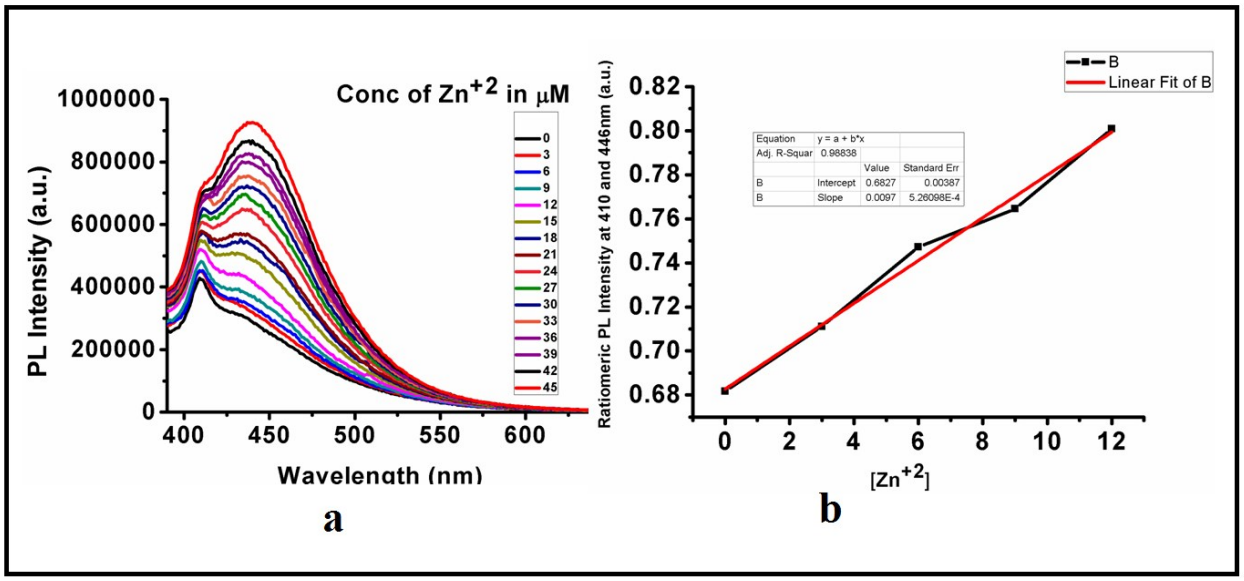

Fig.S14(a) The luminescent spectral changes of **2** MeOH with [M] = 10^{-6} mol L^{-1} upon gradual increasing concentration of $Zn(NO_3)_2$; (b) a linear fitting was obtained between concentration range from 0 to 12μ M in methanol vs. PL intensity

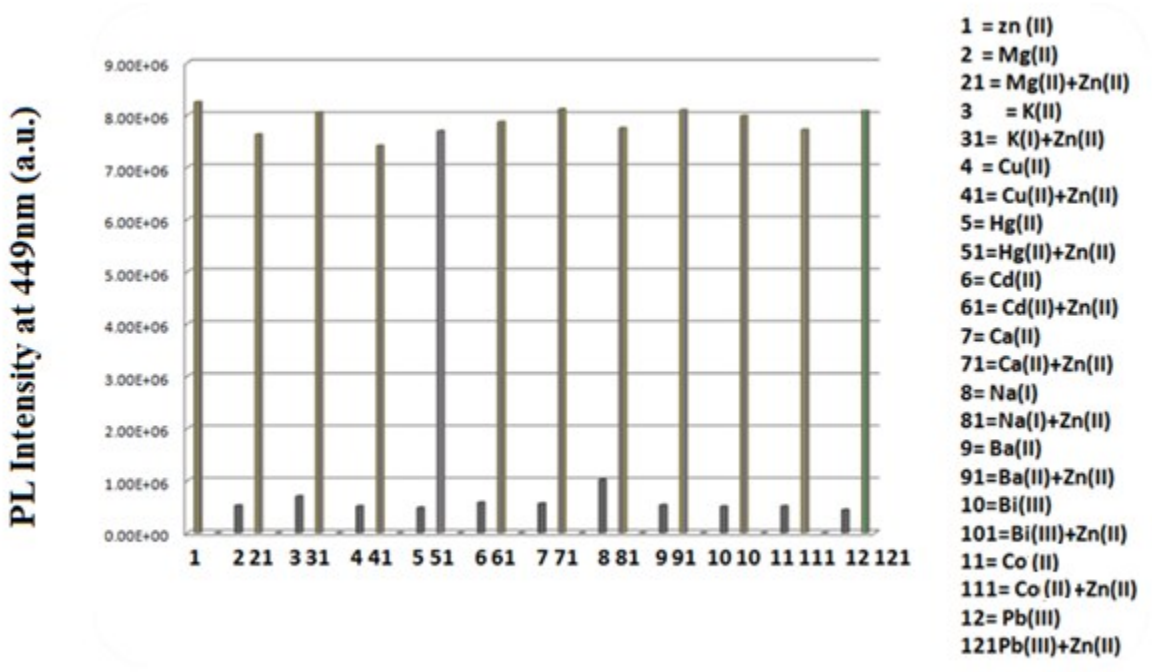

Fig.S15 The comparative fluorescent intensity at 449 nm of mixture of compound **2** with (1 μM MeOH) various salt solutions in MeOH (10equiv) and the mixtures with Zn(II) salt(λ_{ex} = 365 nm, λ_{em} = 449 nm).

Table S1: Crystal data and structure refinement for **2** at 293K.

Empirical formula	$C_{28}H_{26}N_2O$
Formula weight	406.51
Temperature/K	293
Crystal system	Triclinic
Space group	P-1
a/Å	8.6938(3)
b/Å	9.22050(10)
c/Å	14.9549(13)
α/°	75.860(19)
β/°	85.34(2)
γ/°	67.887(16)
Volume/Å^3	1076.90(18)
Z	2
ρ_{calc}g/cm^3	1.254
μ/mm^{-1}	0.076
F(000)	432.0
Crystal size/mm^3	0.2 × 0.2 × 0.2
Radiation	MoKα (λ = 0.71075)
2Θ range for data collection/°	6.19 to 54.968
Index ranges	$-11 \le h \le 11$, $-11 \le k \le 11$, $-19 \le l \le 19$
Reflections collected	11595
Independent reflections	4902 [R_{int} = 0.0442, R_{sigma} = 0.0458]
Data/restraints/parameters	4902/0/285
Goodness-of-fit on F^2	1.076
Final R indexes [I>=2σ (I)]	R_1 = 0.0494, wR_2 = 0.1290
Final R indexes [all data]	R_1 = 0.0641, wR_2 = 0.1426
Largest diff. peak/hole / e Å^{-3}	0.26/-0.18

TableS2: Crystal data and structure refinement for **2b** at 293K..

Empirical formula	$C_{56}H_{52}N_4O_2Zn$
Formula weight	878.38
Temperature/K	293(2)
Crystal system	Triclinic
Space group	P-1
a/Å	13.339(4)
b/Å	13.342(4)
c/Å	15.359(5)
α/°	95.814(3)
β/°	109.924(7)
γ/°	112.425(9)
Volume/Å^3	2289.8(12)
Z	2
ρ_{calc}g/cm^3	1.274
μ/mm^{-1}	0.583
F(000)	924.0
Crystal size/mm^3	0.1 × 0.1 × 0.1
Radiation	MoKα (λ = 0.71075)
2Θ range for data collection/°	6.166 to 54.976
Index ranges	$-17 \le h \le 17$, $-17 \le k \le 17$, $-19 \le l \le 19$
Reflections collected	25027
Independent reflections	10469 [R_{int} = 0.0908, R_{sigma} = 0.1280]
Data/restraints/parameters	10469/0/568
Goodness-of-fit on F^2	1.054
Final R indexes [I>=2σ (I)]	R_1 = 0.0853, wR_2 = 0.1445
Final R indexes [all data]	R_1 = 0.1796, wR_2 = 0.1919
Largest diff. peak/hole / e Å^{-3}	0.46/-0.38

TableS3: Vertical Excitation Energies and Corresponding Orbital Contributions of **2**

Transition from S_0 state to lowest excited states	Experimental Absorbance(nm)	λ_{cal}(nm)	E_{cal}(eV)	Oscillator strength(f)	Assignments (Orbital contribution)
S_1	315	290	4.27	0.5148	HOMO → LUMO (91.39%)
S_2	255	236	5.24	0.0224	HOMO-1 → LUMO (63.82%) HOMO → LUMO (2.54%)
S_3	228	228	5.43	0.3064	HOMO-6 → LUMO (56.84%)

Table S4. It shows the H-bonding interactions and short-contacts (Å) present within a molecule, within a molecular pair and between molecular pairs (a, for the structure collected at rt; b, the structure collected at liq. N_2temperature)

a

S. No	Type of interactions	Within a molecule	Within molecular pair interactions	Molecular pair to molecular pair interactions
1	Hydrogen bond	N1...H1 = 1.890 Å	---	---
2	Inequivalent short contacts	---	C5...H21= 2.873 Å H8...H8 = 2.357 Å	C5...H9 = 2.882 Å C25...H13 = 2.752 Å

b

S. No	Type of interactions	Within a molecule	Within molecular pair interactions	Molecular pair to molecular pair interactions
1	Hydrogen bond	N1...H1 = 1.899 Å	---	---
2	Inequivalent short contacts	---	C5(A)...H21(B) = 2.845Å H8(A)...H8(B) = 2.356 Å	H14(A)...C20(B) = 2.899 Å H14(A)...C21(B) = 2.892 Å H24(B)...C14(A)= 2.835 Å H24(B)...H14(A) = 2.367 Å